Far-Infrared, Raman, and Dispersed Fluorescence Spectra, Vibrational Potential Energy Surface, and the Anomeric Effect of 1,3-Benzodioxole

S. Sakurai, N. Meinander,[†] K. Morris, and J. Laane*

Contribution from the Department of Chemistry, Texas A&M University, College Station, Texas 77843

Received December 28, 1998

Abstract: The far-infrared and Raman spectra of 1,3-benzodioxole vapor have been recorded and analyzed. Forty-one infrared and six Raman bands were assigned to transitions between the various ring-puckering energy levels in the ground and excited ring-flapping states. The determination of the energy levels was assisted by analysis of the single vibronic level fluorescence spectra of the jet-cooled molecules. The puckering levels change substantially in the flapping excited state, indicating substantial interaction between the two vibrational modes. From the spectroscopic data, a two-dimensional vibrational potential energy surface was determined. This has a barrier to planarity of 164 cm^{-1} and energy minima at puckering and flapping angles of $\pm24°$ and $\mp3°$, respectively. This molecule has a lower barrier to planarity than 1,3-dioxole, reflecting the influence of the benzene ring on the anomeric effect. Nevertheless, the anomeric effect is clearly the origin of the nonplanarity of this bicyclic ring system.

Introduction

The anomeric effect was first identified as an anomalous effect on sugar conformations but is now recognized as having much broader relevance to conformational and kinetic processes.[1] The anomeric effect[1−4] is present in molecules which have electronegative atoms with lone pairs of electrons in the 1 and 3 positions, as in 1,3-dioxole (**I**). For molecules such as **I**, the effect is believed to arise from the interaction between the nonbonded oxygen p orbitals and the empty σ*(C−O) orbital involving the other oxygen atom. Although numerous cases of conformational preferences have been rationalized on the basis of the anomeric effect, quantitative experimental determinations of its magnitude have not been readily achieved.

In 1993, we reported the low-frequency vibrational study of 1,3-dioxole[5] (**I**), which we believe represents one of the best experimental determinations of the magnitude of the anomeric effect. Analysis of the far-infrared and Raman data made it possible to determine the ring-puckering potential energy function, which showed the molecule to have a bent conformation with a barrier to planarity of 275 cm^{-1} (3.31 kJ/mol) and a dihedral angle of $\pm24°$. Cyclopentene (**II**) is also nonplanar with a similar barrier (232 cm^{-1}), and this arises from the torsional interaction between the methylene groups, which prefer

to bend away from the eclipsed arrangement present for a planar structure.[6] Since these torsional interactions are not present in 1,3-dioxole, this molecule may be expected to be planar, as is 2,5-dihydrofuran[7] (**III**), for example. However, the presence of the electronegative oxygen atoms in the 1,3 positions gives rise to the anomeric effect, and the molecule becomes puckered in order to achieve better overlap between the oxygen nonbonded orbital and the σ*(C−O) orbital (see Figure 5 of ref 5).

I   II   III   IV   V
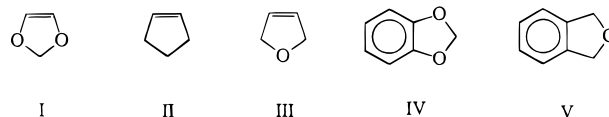
For 1,3-dioxole, we compared the ring-puckering potential energy function determined experimentally to that predicted by the MM3 molecular mechanics program.[8] The molecule was incorrectly predicted by MM3 to be planar. However, agreement between the experimental and calculated barriers to planarity was achieved by utilizing a 2-fold torsional potential energy term, V_2, for internal rotation about the C−O bonds, with a magnitude of −5.97 kcal/mol. This value then can be considered to be a measure of the anomeric effect for this molecule.

In the present study, we extend our investigation to 1,3-benzodioxole (**IV**) to determine the effect that the proximity of the benzene ring has on the anomeric effect. The far-infrared

† Permanent address: Department of Physics, P.O. Box 9, University of Helsinki, Helsinki FIN-00014, Finland.
(1) Kirby, A. J. *The Anomeric Effect and Related Stereolectric Effects at Oxygen*; Springer-Verlag: Berlin, 1983.
(2) Limieux, R. U. P. de May, Ed. *Molecular Rearrangements*; Interscience: New York, 1964; Vol. 2.
(3) Tvaroska, I.; Bleha, T. *Anomeric and Exo-Anomeric Effects in Carbohydrate Chemistry*; Tyson, R. S., Horton, D., Eds.; Academic Press: New York, 1989; Vol. 47.
(4) Szarek, W. A.; Horton, D., Eds. *The Anomeric Effect: Origin and Consequences*; ACS Symposium Series 87; American Chemical Society: Washington, DC, 1979.
(5) Cortez, E.; Verastegui, R.; Villarreal, J. R.; Laane, J. *J. Am. Chem. Soc.* **1993**, *115*, 12132−12136.

(6) (a) Laane, J.; Lord R. C. *J. Chem. Phys.* **1967**, *47*, 4941−4945. (b) Villarreal, J. R.; Bauman, L. E.; Laane, J. *J. Phys. Chem.* **1976**, *80*, 1172−1177. (c) Villarreal, J. R.; Bauman, L. E.; Laane, J. *J. Chem. Phys.* **175**, *63*, 3727−3730. (d) Bauman, L. E.; Killough, P. M.; Cooke, J. M.; Villarreal, J. R.; Laane, J. *J. Phys. Chem.* **1982**, *86*, 2000−2006.
(7) (a) Ueda, T.; Shimanouchi, T. *J. Chem. Phys.* **1967**, *47*, 4042−4047. (b) Carreira, L. A.; Mills, I. M.; Person, W. B. *J. Chem. Phys.* **1972**, *56*, 1444−1448.
(8) Burkert, U.; Allinger, N. L. *Molecular Mechanics*; American Chemical Society Monograph 177; American Chemical Society: Washington, DC, 1982.

spectra of the ring-puckering vibration of 1,3-benzodioxole have been previously reported,[9] but these were recorded at relatively poor resolution (1.3 cm^{-1}), and, as will be shown, the assignments and potential energy function were not correctly determined. More recently, the microwave spectrum of 1,3-benzodioxole was analyzed.[10] In this work, the previously published far-infrared results were also reanalyzed, and a two-dimensional vibrational potential energy surface in terms of ring-puckering and ring-flapping coordinates was calculated. This had a barrier to planarity of 126 cm^{-1}. This result was clearly an improvement, and many of the assignments are, indeed, the correct ones. However, the analysis was nonetheless based, to a large degree, on the old far-infrared data, and, hence, the potential energy surface and barrier to planarity calculated are not very accurate.

In our study, we have recorded improved far-infrared spectra at higher resolution, new vapor-phase Raman spectra, and also dispersed fluorescence spectra in order to accurately determine the principal ring-puckering and ring-flapping energy states. We then applied the methodology recently developed for the analysis of phthalan[11,12] (**V**) in order to calculate the two-dimensional kinetic energy function and potential energy surface for 1,3-benzodioxole.

Experimental Section

1,3-Benzodioxole (99% purity) was purchased from Aldrich Chemical. Far-infrared spectra of samples were taken using a Bomem DA 8.02 Fourier transform spectrometer equipped with a variable path length multipass cell from Infrared Analysis. A helium-cooled bolometer was used as the detector. Raman spectra were collected using an ISA U-1000 double monochromator with a Coherent argon ion laser operating at 514.5 nm or a Coherent DPSS Nd:YAG laser operating at 532 nm as the excitation source. The special cells previously described[13] were used to collect the Raman spectra of vapors at 200 °C. A charge-coupled device (CCD) or photomultiplier tube was used as the detector. Dispersed fluorescence spectra of jet-cooled molecules were collected using an apparatus and Nd:YAG pumped dye laser system described elsewhere.[14] Spectral lines were separated using an ISA HR640 monochromator and detected with a photomultiplier detector.

Results and Discussion

The far-infrared spectrum of 1,3-benzodioxole vapor is shown in Figure 1, and the high-temperature vapor-phase Raman spectrum is presented in Figure 2. Figure 3 shows the dispersed fluorescence spectrum of the jet-cooled molecules collected from the electronic band origin at 34 788 cm^{-1}. Table 1 presents a listing of our observed far-infrared frequencies and intensities and compares these to those reported by Duckett, Smithson, and Wieser[9] (DSW). Table 2 lists the Raman data for the ring-puckering double-quantum transitions and the ring-flapping and twisting fundamentals. Table 3 presents the ground-state energy levels calculated from the far-infrared spectra and compares
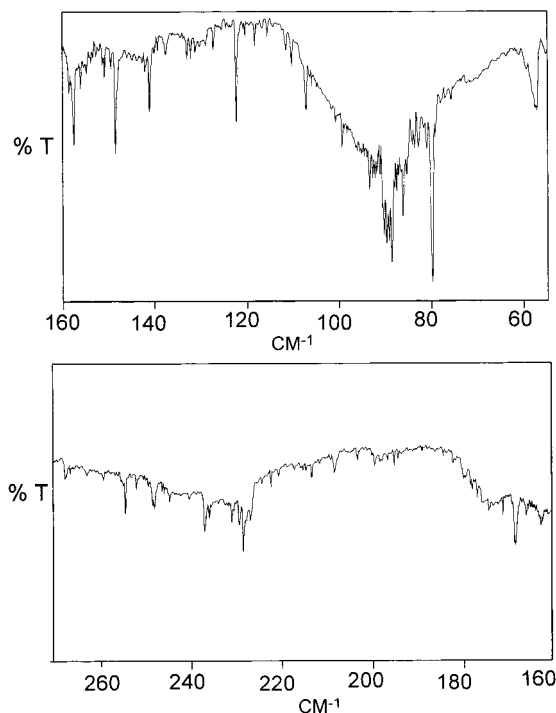
(9) Duckett, J. A.; Smithson, T. L.; Wieser, H. *Chem. Phys. Lett.* **1979**, *64*, 261−264.

(10) Caminati, W.; Melandri, S.; Corbelli, G.; Favero, L. B.; Meyer R. *Mol. Phys.* **1993**, *80*, 1297−1315.

(11) Klots, T.; Sakurai, S.; Laane, J. *J. Chem. Phys.* **1998**, *108*, 3531−3536.

(12) Sakurai, S.; Meinander, N.; Laane, J. *J. Chem. Phys.* **1998**, *108*, 3537−3542.

(13) Haller, K.; Chiang, W.-Y.; del Rosario, A. *J. Mol. Struct.* **1996**, *379*, 19−23.

(14) (a) Cheatham, C. M.; Huang, M.-H.; Laane, J. *J. Mol. Struct.* **1996**, *377*, 93−99. (b) Cheatham, C. M.; Huang, M.-H.; Meinander, N.; Kelly, M. B.; Haller, K.; Chiang, W.-Y.; Laane, J. *J. Mol. Struct.* **1996**, *377*, 81−92. (c) Morris, K. Ph.D. Thesis, Texas A&M University, College Station, TX, 1998.

Figure 1. Far-infrared spectra of 1,3-benzodioxole. Vapor pressure, 0.5 Torr; path length, 20 m; resolution, 0.25 cm^{-1}. Top, 55−160 cm^{-1}; bottom, 160−270 cm^{-1}.

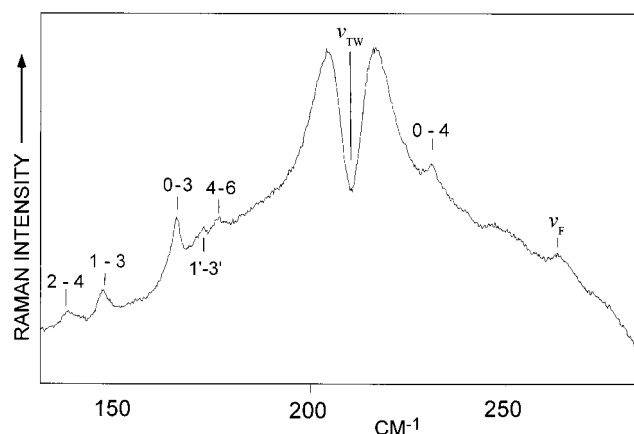**Figure 2.** Vapor-phase Raman spectrum of 700 Torr of 1,3-benzodioxole at 200 °C. Quantum numbers are shown for the puckering transitions. Primes correspond to the $v_F = 1$ state. v_{TW} = ring twisting; v_F = ring flapping.

these to values determined from the dispersed fluorescence spectra. Average values from a dozen spectra involving different excitation bands are given. The table also lists previously reported dispersed fluorescence frequencies reported by Hassan and Hollas[15] (HH). However, the HH assignments are very different from ours, as they utilized the DSW data and incorrectly assumed the molecule to have a twisted structure. Figure 4 shows the energy level diagram for the ring-puckering and ring-flapping quantum states along with some of the observed transition frequencies. These energy levels are totally different from those reported by DSW but are fairly similar to those proposed by Caminati et al.[10] (CMCFM). They differ substantially from the CMCFM assignments for the $v_F = 1$ flapping state, where the $v_P = 0$ and $v_P = 1$ states were assumed by CMCFM to be at 236.4 and 252.3 cm^{-1} instead of 267.2

(15) Hassan, K. H.; Hollas, J. M. *Chem. Phys. Lett.* **1989**, *157*, 183−188.
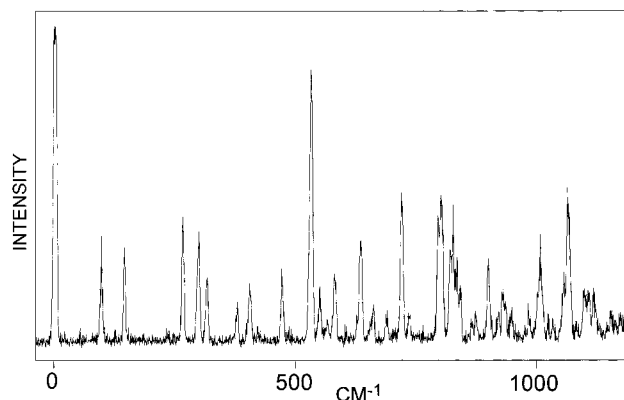
Figure 3. Dispersed fluorescence spectra from the 0_0^0 band of jet-cooled 1,3-benzodioxole.

and 297.8 cm^{-1}, respectively. This is significant in that we observe that the splitting in the flapping excited state has increased from the 9.1 cm^{-1} value in the ground state to 30.6 cm^{-1}. CMCFM assumed the change to go from 8.1 to 15.9 cm^{-1}. For the CMCFM assignment to be valid, the $(v_F, v_P) = (1,0)$ level would have to be within 1 cm^{-1} of the $v_P = 4$ level at 236.8 cm^{-1}, and we see no evidence of that. Moreover, the CMCFM assignment cannot account for the levels at 267 and 298 cm^{-1} (Table 3), although DSW assign the latter band to v_{14}, a ring-bending mode. Furthermore, the Raman spectrum of liquid 1,3-benzodioxole shows depolarized bands at 226 and 285 cm^{-1}, which we assign to $v_{20}(A_2)$, the ring twisting, and $v_{38}(B_2)$, the ring flapping, respectively. The vapor-phase Raman band (Figure 2) at 214 cm^{-1} clearly corresponds to v_{20} on the basis of its band type. Hence, the flapping frequency for the vapor is expected to be about 60 cm^{-1} higher, or near 270 cm^{-1}. The MM3 calculation predicts v_{20} and v_{38} to be at 294 and 391 cm^{-1}, respectively. Both values are considerably higher than observed, but the relative frequencies are reasonable. For the $v_{14}(A_1)$ ring angle bending mode, the MM3 calculation predicts a value of 498 cm^{-1}, and we assign this to a polarized Raman band for the liquid at 537 cm^{-1}. The only other low-frequency vibrations which need to be considered are $v_{37}(B_2)$, a benzene ring-bending mode, which is assigned to an infrared band at 409 cm^{-1}, and $v_{32}(B_1)$, a ring-bending mode of the five-membered ring, which is calculated to be at 391 cm^{-1}. The v_{32} infrared band, however, should have a type B band contour without a sharp center branch, so this will not be easily confused with any of the bands assigned in Table 1. A more complete analysis of the vibrational assignments will be presented elsewhere.[16]

As can be seen in Tables 1 and 2, the 41 observed far-infrared and seven observed Raman frequencies, along with the dispersed fluorescence data in Table 3, define the ring-puckering and ring-flapping energy levels shown in Figure 4 with a high degree of certainty, and these then were utilized to determine the potential energy surface governing these two motions. It should be noted that there are five important spectral bands between 88 and 91 cm^{-1} which are critical to the assignments. With their poorer resolution, DSW reported only one band at 89.0 cm^{-1}.

The calculations for the potential energy surfaces were carried out using methodology we have developed over many years of work.[17-20] The ring-puckering and ring-flapping coordinates are

(16) Sakurai, S.; Laane, J. *J. Mol. Struct.*, in press.

(17) Laane, J. *Annu. Rev. Phys. Chem.* **1994**, *45*, 179−211.

(18) Laane, J. In *Structures and Conformations of Non-Rigid Molecules*; Laane, J., Dakkouri, M., van der Veken, B., Oberhammer, H., Eds.; Kluwer: Dordrecht, The Netherlands, 1993; pp 65−98.

(19) Laane, J. *Pure Appl. Chem.* **1987**, *59*, 1307−1326.

Table 1. Far-Infrared Spectral Bands of 1,3-Benzodioxole

		this work		DSW[d]	
	transition[a]	v (cm^{-1})[b]	inferred[c]	v (cm^{-1})	assignment
$\Delta v_P = 1$	$(0,0) \rightarrow (0,1)$		9.6		
	$(0,1) \rightarrow (0,2)$	89.5 s		89.0	$(1,0) \rightarrow (0,2)$
	$(0,2) \rightarrow (0,3)$	58.2 s		59.0	hot band
	$(0,3) \rightarrow (0,4)$	79.5 s		80.0	hot band
	$(0,4) \rightarrow (0,5)$	88.4 s		89.0	$(1,0) \rightarrow (0,2)$
	$(0,5) \rightarrow (0,6)$	90.0 ms			
	$(0,6) \rightarrow (0,7)$	93.2 mw			
	$(1,0) \rightarrow (1,1)$		30.6		
	$(1,1) \rightarrow (1,2)$	85.9 m		86.0	hot band
	$(1,2) \rightarrow (1,3)$	88.9 ms			
	$(1,3) \rightarrow (1,4)$	90.9 w			
$\Delta v_P = 2$	$(0,0) \rightarrow (0,2)$	98.8 vw	98.6	99.2	hot band
	$(0,1) \rightarrow (0,3)$	148.2 s	147.7	148.5	hot band
	$(0,2) \rightarrow (0,4)$	137.2 mw	137.7		
	$(0,3) \rightarrow (0,5)$	167.6 ms	167.9	167.8	$(0,1) \rightarrow (0,2)$
	$(0,4) \rightarrow (0,6)$	178.7 w	178.4		
	$(0,5) \rightarrow (0,7)$	183.6 vvw	183.2		
	$(1,0) \rightarrow (1,2)$	116.4 vvw	116.5		
	$(1,1) \rightarrow (1,3)$	174.8 w	174.7		
	$(1,2) \rightarrow (1,4)$	181.3 vw	180.8		
$\Delta v_P = 3$	$(0,0) \rightarrow (0,3)$	157.3 vs	157.3	157.6	$(0,0) \rightarrow (0,1)$
	$(0,1) \rightarrow (0,4)$	227.8 s	227.8	228.1	hot band
	$(0,2) \rightarrow (0,5)$	226.3 vvw	226.1	226.6	hot band
	$(0,3) \rightarrow (0,6)$	258.8 w	257.9	259.3	hot band
$\Delta v_P = 4$	$(0,0) \rightarrow (0,4)$	236.4 m	236.8	236.4	$(0,0) \rightarrow (1,0)$
$\Delta v_F = \pm 1$	$(0,0) \rightarrow (1,0)$	267.2 mw		266.4	sum band
	$(1,0) \rightarrow (2,0)$	262.4 w		262.8	hot band
	$(0,0) \rightarrow (1,1)$	297.8 m		298.0	v_{14}
	$(0,1) \rightarrow (0,0)$	overlap	258.1		
	$(0,1) \rightarrow (1,1)$	289.5 vw	288.2		
	$(0,2) \rightarrow (1,0)$	158.3 mw	158.1		
	$(0,2) \rightarrow (1,1)$	198.7 w	198.7		
	$(0,2) \rightarrow (1,2)$	285.1 vvw	284.6		
	$(0,3) \rightarrow (1,0)$	109.9 w	109.9		
	$(0,3) \rightarrow (1,1)$	140.7 s	140.5	141.1	difference band
	$(0,3) \rightarrow (1,2)$	overlap	226.4		
	$(0,3) \rightarrow (1,3)$	315.8 w	315.3		
	$(0,4) \rightarrow (1,0)$		30.4		
	$(0,4) \rightarrow (1,1)$	60.1 w	61.0		
	$(0,4) \rightarrow (1,2)$	~146.7 w	146.9		
	$(0,4) \rightarrow (1,3)$	235.4 w	235.9		
	$(0,4) \rightarrow (1,4)$	327.5 w	327.7		
	$(0,1) \rightarrow (0,5)$	overlap	58.0		
	$(1,1) \rightarrow (0,5)$		27.4		
	$(0,5) \rightarrow (1,2)$	overlap	58.5		
	$(0,5) \rightarrow (1,3)$	overlap	147.4		
	$(0,5) \rightarrow (1,4)$	239.6 vw	239.3		
	$(1,0) \rightarrow (0,6)$	overlap	148.0		
	$(1,1) \rightarrow (0,6)$	117.9 mw	117.4		
	$(1,2) \rightarrow (0,6)$		31.5		
	$(0,6) \rightarrow (1,3)$	overlap	57.4		
	$(0,6) \rightarrow (1,4)$	149.1	149.3		
	$(1,0) \rightarrow (0,7)$		241.2		
	$(1,1) \rightarrow (0,7)$	210.8	210.6		

[a] The levels are given by (v_F, v_P). [b] s, strong; m, medium; w, weak; v, very. [c] Inferred values are calculated from $\Delta v_P = 1$ far-infrared transitions whenever possible. [d] Reference 9.

defined in Figure 1 of ref 11. Recently, we have applied these methods to the analysis of phthalan[11,12] (**V**), which was found to have a very small barrier to planarity of 35 cm^{-1}. For phthalan, the spectra were complicated by the large interaction between the ring-puckering and ring-flapping modes, which made a one-dimensional analysis of the ring-puckering vibration impractical. For 1,3-benzodioxole, we first utilized a one-dimensional potential energy function to best fit the experimental data. Based on the molecular structure and assumed vibrational

(20) Laane, J. *J. Mol. Struct.* **1985**, *126*, 99−100.

Spectral Study of 1,3-Benzodioxole

J. Am. Chem. Soc., Vol. 121, No. 21, 1999 5059

Table 2. Raman Spectral Bands of 1,3-Benzodioxole

transition	Raman frequency (cm^{-1})	inferred[a]
$(0,1) \rightarrow (0,3)$	147.9	147.7
$(0,2) \rightarrow (0,4)$	138.5	137.7
$(0,3) \rightarrow (0,5)$	167.9	167.9
$(0,4) \rightarrow (0,6)$	178.7	178.4
$(0,0) \rightarrow (0,4)$	235.9	236.8
$(0,0) \rightarrow (1,0)$	263.8	267.2
v_{TWIST}	214.0	

[a] From far-infrared transitions.

model, the one-dimensional kinetic energy function was found to be

$$g_{44} = 0.006718 - 0.0542x_1^2 + 0.1833x_1^4 - 0.6119x_1^6 \quad (1)$$

where x_1 (in Å) is the ring-puckering coordinate.[11,12] The potential energy function which gave the best fit to the experimental data using this g_{44} function above was determined to be

$$V(\text{cm}^{-1}) = (1.292 \times 10^6)x_1^4 - (2.573 \times 10^4)x_1^2 \quad (2)$$

Figure 5 shows this function and also compares the observed vibrational frequencies to those calculated using this function. The agreement is not too bad, but it begins to get worse for the higher transitions. Moreover, the one-dimensional model cannot be used to represent the large change in frequency separations found in the flapping excited ($v_F = 1$) state. The barrier to planarity for this one-dimensional calculation is 128 cm^{-1}, which is similar to the 126 cm^{-1} value reported by CMCFM.

To analyze all of the energy states in Figure 4 and to understand the interaction between the two conformationally important vibrational modes, a two-dimensional potential energy surface which fits all the data was determined. First, the two-dimensional kinetic energy expansions[11,12] in terms of the puckering (x_1) and flapping coordinates (x_2) were calculated:

$$g_{44} = 0.010051 - 0.16875x_1^2 + 1.7290x_1^4 - 14.9557x_1^6 -$$
$$0.018393x_2^2 + 0.282863x_2^4 - 1.0264x_2^6 +$$
$$0.170831x_2^2x_3^3 + 0.28286x_1^2x_2^3 + 1.02636x_1^2x_2^3 \quad (3)$$

$$g_{45} = 0.130578 - 0.0040853x_1^2 + 6.81894x_1^4 -$$
$$83.09016x_1^6 - 0.1496885x_2^2 + 0.1276195x_2^4 -$$
$$0.3156069x_2^6 + 0.832740x_2^2x_2^3 + 0.2062571x_1^2x_2^3 +$$
$$0.0208667x_1^2x_2^3 \quad (4)$$

$$g_{55} = 0.020376 - 0.23319x_1^2 + 1.65439x_1^4 -$$
$$14.4207x_1^6 - 0.014229x_2^2 + 0.39786x_2^4 - 1.44954x_2^6 +$$
$$0.36573x_2^2x_2^3 + 0.118277x_1^2x_2^3 + 0.131152x_1^2x_2^3 \quad (5)$$

Here, g_{44} represents the coordinate-dependent reciprocal reduced mass for the ring-puckering, while g_{55} and g_{45} correspond to the ring-flapping and interaction between the two modes, respectively. Graphical representation of these surfaces is shown in Figures 6−8. The coordinate dependence can be seen to be substantial, and it must be considered for meaningful calculations.

Two potential energy surfaces, both of which do a respectable job of fitting the data, were calculated. The first was constrained to have only even powered terms in x_1 and x_2. This form of the

Table 3. Energy Levels of 1,3-Benzodioxole Determined from Far-Infared and Dispersed Fluorescence Spectra

level[a]	sym	inferred[b]	SVLF[c] this work	HH[d]	CMCFM[e]
$(0,1)$	B_2	9.6	9		30 ± 30
$(0,2)$	A_1	99.1	100	102	70 ± 40
$(0,3)$	B_2	157.3	154	153	220 ± 60
$(0,4)$	A_1	236.8	238	234	
$(0,5)$	B_2	325.2	317		
$(1,0)$	B_2	267.2	267		
$(1,1)$	A_1	297.8	299	300	
$(1,2)$	B_2	383.7	380		
$(1,3)$	A_1	427.6	477		
v_{37}	B_2		405		
$2v_{TW}$	A_1	428	422	425	
v_{14}	A_1	537	536	536	
v_{13}	A_1	736	735	716	
v_{12}	A_1	799	799	800	
v_{11}	A_1	824	832		
v_{10}	A_1	1003	1006	1004	
v_9	A_1	1051	1060		

[a] (v_F, v_P) or the vibration number is indicated; $v_{TW} = v_{20}$. [b] From far-infrared data. [c] SVLF = single vibronic level fluorescence; average values from dispersed fluorescence spectra recorded from several different excitation frequencies. [d] Reference 15. [e] Reference 10.

surface requires that the energy minima occur where the flapping coordinate (x_2) is equal to zero. In the second calculation, odd power terms were included. The first calculation resulted in the potential energy surface

$$V(\text{cm}^{-1}) = (1.929 \times 10^6)x_1^4 - (3.557 \times 10^4)x_1^2 +$$
$$(6.033 \times 10^3)x_2^2 + (2.806 \times 10^5)x_1^2x_2^2 \quad (6)$$

This has a barrier to planarity of 164 cm^{-1} and energy minima at $x_1 = \pm 0.096$ Å, which correspond to dihedral angles of puckering of $\pm 21°$. This potential energy surface is shown in Figure 9. The comparison between experimental and calculated frequencies for this surface is given in Table 4 as "calc I", and the agreement can be seen to be good. The change in the splitting between the puckering levels for the $v_F = 0$ and $v_F = 1$ states is nicely reproduced.

The frequency fit can be improved somewhat by the addition of an x_1x_2 term. The resulting potential surface is

$$V(\text{cm}^{-1}) = (1.502 \times 10^6)x_1^4 - (2.971 \times 10^4)x_1^2 +$$
$$(6.956 \times 10^3)x_3^3 + (8.312 \times 10^5)x_1x_2 +$$
$$(2.661 \times 10^5)x_1^2x_2^2 \quad (7)$$

and the frequencies calculated ("calc II") for this surface are also shown in Table 4. This surface also has a barrier of 164 cm^{-1} and is shown in Figure 10. It looks similar to that in Figure 9, except that the minima are moved slightly off of the x_1 axis. The energy minima are at $x_1 = \pm 0.102$ Å, $x_2 = \mp 0.044$ Å, corresponding to puckering and flapping angles of $\pm 24°$ and $\mp 3°$, respectively. The microwave analysis by CMCFM, which also considered the rotational constants with vibrational state, reached a similar conclusion, that the molecule possesses not only a puckered structure but also one with a small degree of flapping. These workers reported puckering and flapping angles of 26.8° and 8.3°, respectively. Our analysis of the far-infrared data shows that "calc II" (eq 7) gives somewhat better results than "calc I" (eq 6), but the improvement is only modest. Hence, the small flapping angle calculated lies within the experimental uncertainty. Namely, it is $3 \pm 3°$. However, we believe the
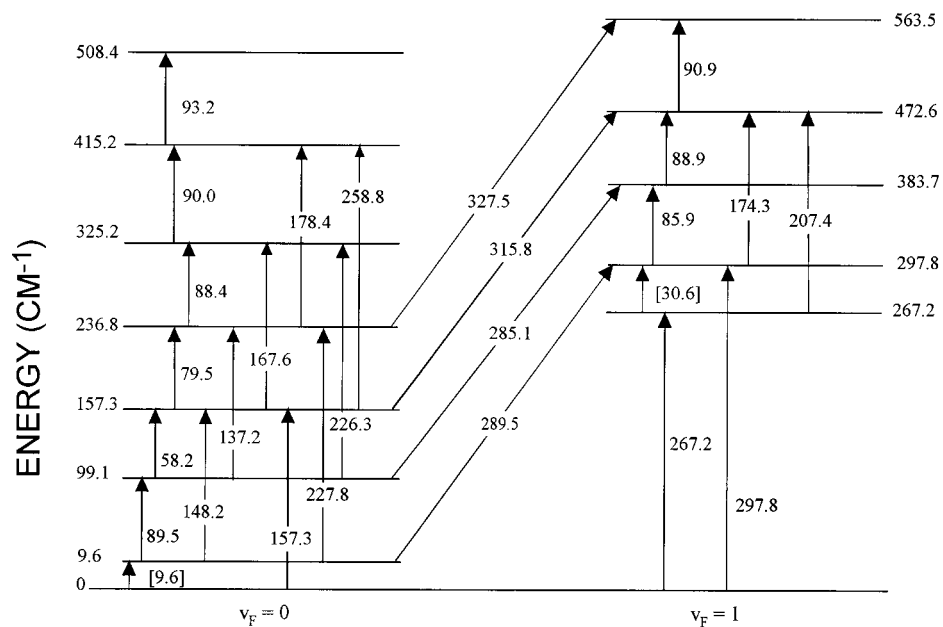
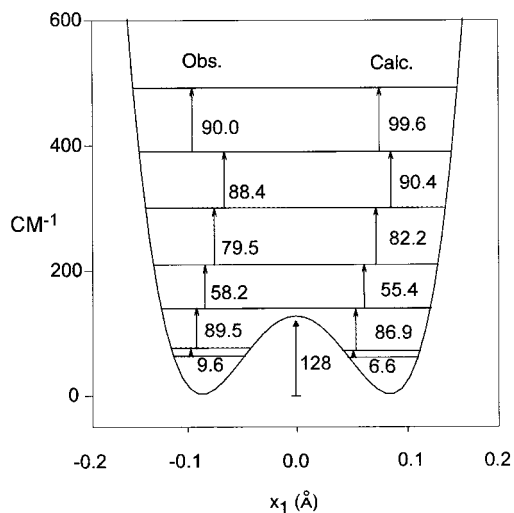**Figure 4.** Energy level diagram for the ring-puckering and ring-flapping vibrations of 1,3-benzodioxole.

Figure 5. One-dimensional potential energy function calculated for the ring-puckering of 1,3-benzodioxole.
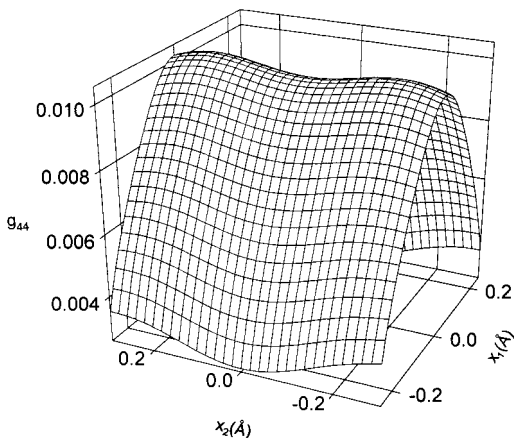

Figure 6. Coordinate dependence of g_{44} (au^{-1}), the reciprocal reduced mass for the ring-puckering motion.

barrier to planarity to be quite accurate, at 164 ± 5 cm^{-1}, and the puckering angle is $24° \pm 3°$. It should be noted that, for molecules such as 1,3-benzodioxole, the puckering motion has an amplitude of more that $\pm 10°$ from its energy minima. Thus,
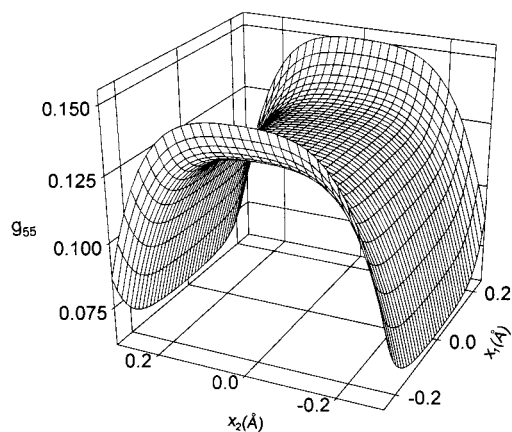
Figure 7. Coordinate dependence of g_{55} (au^{-1}), the reciprocal reduced mass for the ring-flapping motion.
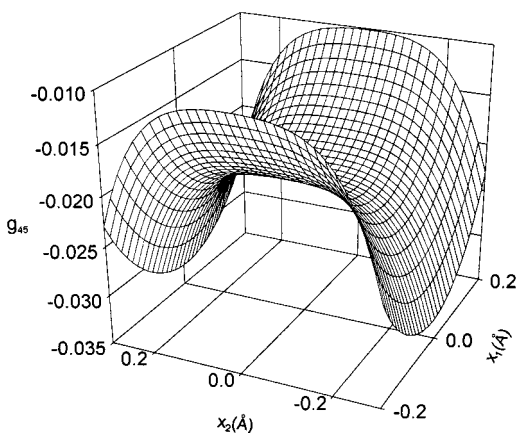

Figure 8. Coordinate dependence of g_{45} (au^{-1}), the kinetic energy interaction term.

the potential energy minima do not exactly correspond to the average puckering angle. Table 4 also lists the calculated frequencies from the one-dimensional calculation (eq 2), and these can be seen to be considerably worse than those calculated using either two-dimensional calculation.

The principal conclusion from these results is that the lower barrier of 1,3-benzodioxole (**IV**) as compared to that of 1,3-
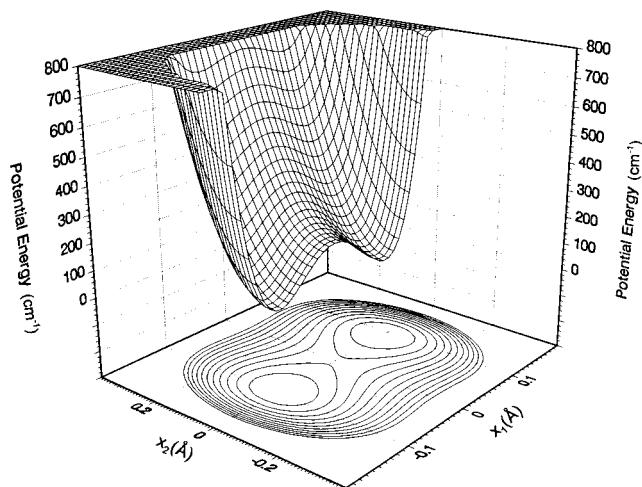
Figure 9. Two-dimensional potential energy surface for the ring-puckering and ring-flapping vibrations of 1,3-benzodioxole (calc I).

Table 4. Observed and Calculated Frequencies of 1,3-Benzodioxole

transition	obsd	calc I[a]	Δ	calc II[b]	Δ	calc III[c]	Δ
$(0,0) \rightarrow (0,1)$	9.6	9.7	−0.1	9.7	−0.1	6.6	3.0
$(0,1) \rightarrow (0,2)$	89.5	89.5	0.0	90.1	−0.6	86.9	2.6
$(0,2) \rightarrow (0,3)$	58.2	60.3	−2.1	59.4	−1.2	55.4	2.8
$(0,3) \rightarrow (0,4)$	79.5	83.8	−4.3	83.3	−3.8	82.2	−2.7
$(0,4) \rightarrow (0,5)$	88.4	87.4	1.0	87.1	1.3	90.4	−2.0
$(0,5) \rightarrow (0,6)$	90.0	88.5	0.5	89.3	0.7	99.6	−9.5
$(0,6) \rightarrow (0,7)$	93.2	91.4	1.8	92.0	1.3	107.1	−13.9
$(0,0) \rightarrow (0,1)$	267.2	267.2	0.0	267.3	−0.1		
$(1,0) \rightarrow (1,1)$	30.6	29.7	0.9	30.4	0.2		
$(1,1) \rightarrow (1,2)$	85.9	83.3	2.6	84.2	1.7		
$(1,2) \rightarrow (1,3)$	88.9	90.6	−0.7	87.8	1.1		
$(1,3) \rightarrow (1,4)$	90.9	88.5	2.4	88.0	1.9		
$(1,1) \rightarrow (1,2)$	262.4	252.4[d]	(−9.8)	250.5[d]	(−11.9)		
av Δ			1.4		1.2		5.4
av Δ²			3.4		2.3		45.4

[a] $V \, (\text{cm}^{-1}) = (1.929 \times 10^6)x_1^4 - (3.557 \times 10^4)x_1^2 + (6.033 \times 10^3)x_2^2 + (2.806 \times 10^5)x_1^2x_2^2$. [b] $V \, (\text{cm}^{-1}) = (1.502 \times 10^6)x_1^4 - (2.971 \times 10^4)x_1^2 + (6.956 \times 10^3)x_3^2 + (8.312 \times 10^5)x_1x_2 + (2.661 \times 10^5)x_1^2x_2^2$. [c] One-dimensional calculation. $V = (1.292 \times 10^6)x^4 - (2.573 \times 10^4)x^2$. [d] This calculated number was not used in determining the potential energy surface. It could be adjusted by addition of an x_2^4 term to reflect the observed anharmonicity.
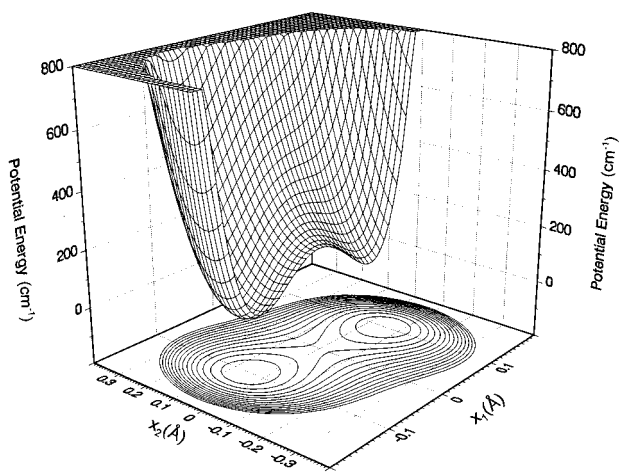

Figure 10. Two-dimensional potential energy surface for the ring-puckering and ring-flapping vibrations of 1,3-benzodioxole (calc II).

dioxole (**I**), 164 vs 275 cm⁻¹, clearly results from the difference between how the benzene ring and the carbon−carbon double bond influence the anomeric effect. The anomeric effect is
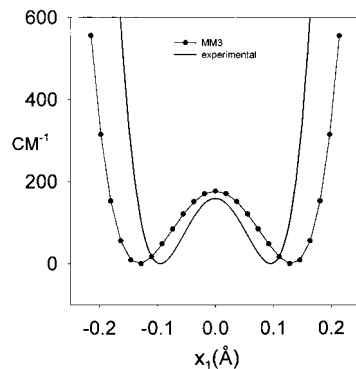

Figure 11. Comparison of the experimental ring-puckering potential energy along the x_1 coordinate with that calculated from the MM3 molecular mechanics program.
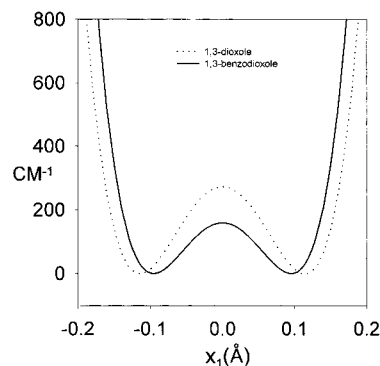

Figure 12. Comparison of the 1,3-benzodioxole and 1,3-dioxole ring-puckering potential energy functions.

clearly the cause of the barrier to planarity since there are no torsional forces between adjacent methylene groups influencing the five-membered ring to become puckered.

When we investigated 1,3-dioxole, we compared our experimentally determined potential energy function with that predicted by a molecular mechanics calculation (MM3). The MM3 result predicted a planar ring system in contrast with the experiment. However, we were able to achieve satisfactory agreement after we introduced the torsional forces expected from the anomeric effect. Specifically, the C−O−C−O torsional constant was increased from −2.00 to −5.695 kcal/mol.

We carried out similar MM3 calculations for 1,3-benzodioxole. Suprisingly, the results gave a reasonable representation without modification of the torsional constant (i.e., leaving V_2 = −2.00 kcal/mol). Figure 11 compares the calculated one-dimensional MM3 potential function to the experimental one (eq 6 with $x_2 = 0$). This shows that the force constant parameters in the MM3 program lead to the prediction that 1,3-benzodioxole is nonplanar, with a barrier to planarity of 177 cm⁻¹. This barrier is slightly higher than the experimental one, and the MM3 potential energy curve represents a more puckered molecule than what has been determined experimentally. Nonetheless, the fairly good agreement between the barrier heights indicates that the MM3 force constants, including V_2 = −2.00 kcal/mol for the C−O−C−O torsion, are quite reasonable. Hence, the anomeric effect is reduced by more than a factor of 2 when compared to that of 1,3-dioxole. Figure 12 compares the 1,3-benzodioxole one-dimensional potential energy function to the function determined for 1,3-dioxole. The higher barrier height and greater degree of puckering of 1,3-dioxole again are indications of the decrease in the anomeric effect in 1,3-benzodioxole.

Conclusions

The complex nature of the vibrational energy levels of 1,3-benzodioxole arising from the ring-puckering and ring-flapping vibrations results from the interaction between these two conformationally important modes. The far-infrared spectra of this molecule show not only the usual single-quantum transitions but also others which can be utilized to determine a detailed energy map of all the lower energy states. In addition, the Raman spectra and dispersed fluorescence spectra provide complementary data on the double-quantum transition frequencies and total energy state values, respectively. This comprehensive understanding of the energy levels is necessary in order to accurately determine the potential energy surface governing the conformational changes in this molecule. This potential energy surface shows that the puckering and flapping motions are intimately coupled and that the molecule has a puckered conformation with a barrier to planarity of 164 cm^{-1}. This barrier arises from the anomeric effect, which results from the presence of the two electronegative oxygen atoms in the 1,3 position. However, as compared to that of 1,3-dioxole, the magnitude of the anomeric effect has been decreased by approximately a factor of 2. Thus, the introduction of the benzene ring adjacent to the oxygen atoms has the effect of reducing the interaction between the oxygen nonbonding p orbitals and the σ*(C—O) orbitals. Recent ab initio calculations corroborate these findings and also agree remarkably well with the magnitudes of the barriers we have experimentally determined for 1,3-benzodioxole and 1,3-dioxane.[21] The ab initio calculation at the MP2/6-31G* level predicts a barrier of 171 cm^{-1} and puckering and flapping angles of 24.2° and 2.6°, respectively, for 1,3-benzodioxole. An earlier ab initio calculation on 1,3-dioxole was also in accord with our findings.[22]

(21) Moon, S.; Kwon, Y.; Choo, J. *J. Mol. Struct. (THEOCHEM)*, in press.
(22) Suarez, D.; Sordo, T. L.; Sordo, J. A. *J. Am. Chem. Soc.* **1996**, *118*, 9850−9854.